Simulations of Extratropical Cyclogenesis with the Unified, Quasi-Hydrostatic and Anelastic Dynamical Cores

Celal Konor

Department of Atmospheric Science
Colorado State University

Tenth CMMAP Team Meeting, 11-13 January 2011, Berkeley, CA
Dynamical Framework Working Group

A dynamical core based on the unified (UN) system has been constructed. The preliminary results are very encouraging

Outline

- A descriptive comparison of the unified (UN), quasi-hydrostatic (QH) and anelastic (AN) dynamical cores
  - Continuous equations
  - Important aspects of discretization of the UN dynamical core
- Simulations of extratropical cyclogenesis on midlatitude β- and f- planes
- A comparison of the results obtained by the three models
- Conclusions

Equations of the Models

Quasi-Hydrostatic	Anelastic	Unified
$\frac{D\mathbf{v}}{Dt}+f\mathbf{k}\times\mathbf{v}$ $+c_p\theta\nabla_H\pi_{qs}=\mathbf{F}_H$	$\frac{D\mathbf{v}}{Dt}+f\mathbf{k}\times\mathbf{v}$ $+c_p\bar{\theta}\nabla_H\pi'=\mathbf{F}_H$	$\frac{D\mathbf{v}}{Dt}+f\mathbf{k}\times\mathbf{v}$ $+c_p\theta\nabla_H\pi_{qs}+c_p\theta\nabla_H\delta\pi=\mathbf{F}_H$
$\pi=\pi_{qs}$	$\pi=\bar{\pi}(z)+\pi' \quad \theta=\bar{\theta}(z)+\theta'$ *Bar: Basic/Mean state prime: Deviation*	$\pi=\pi_{qs}+\delta\pi$ *qs: Quasi-hydrostatic δ: Non-hydrostatic*
$c_p\theta\frac{\partial}{\partial z}\pi_{qs}=-g$ $\left[\frac{1}{\rho_{qs}}\frac{\partial}{\partial z}p_{qs}=-g\right]$	$\frac{Dw}{Dt}+c_p\bar{\theta}\frac{\partial}{\partial z}\pi'-g\frac{\theta-\bar{\theta}}{\bar{\theta}}=F_w$ *Not used in the model*	$\frac{Dw}{Dt}+c_p\theta\frac{\partial}{\partial z}\delta\pi=F_w$ *Not used in the model*
$\frac{D\theta}{Dt}=\frac{Q}{c_p\pi_{qs}}$	$\frac{D\theta}{Dt}=\frac{Q}{c_p\pi}$	$\frac{D\theta}{Dt}=\frac{Q}{c_p\pi}$

Equations of the Models (Cont.)

Quasi-Hydrostatic	Anelastic	Unified
$c_p\theta\frac{\partial}{\partial z}\pi_{qs} = -g$ and $\frac{\partial}{\partial z}p_{qs} = -\rho_{qs}g$ $\frac{\partial}{\partial t}\left(\pi_{qs}\right)_S = H_1$ and $\frac{\partial}{\partial t}\left(\pi_{qs}\right)_T = H_2$	N / A	$c_p\theta\frac{\partial}{\partial z}\pi_{qs} = -g$ and $\frac{\partial}{\partial z}p_{qs} = -\rho_{qs}g$ $\frac{\partial}{\partial t}\left(\pi_{qs}\right)_S = H_1$ and $\frac{\partial}{\partial t}\left(\pi_{qs}\right)_T = H_2$
$\rho_{qs} = \frac{p_{00}\pi_{qs}^{(1-\kappa)/\kappa}}{R\theta}$	N / A	$\rho_{qs} = \frac{p_{00}\pi_{qs}^{(1-\kappa)/\kappa}}{R\theta}$
$\frac{\partial\left(\rho_{qs}w\right)}{\partial z} = -\mathbf{\nabla}_H\cdot\left(\rho_{qs}\mathbf{v}\right) - \frac{\partial\rho_{qs}}{\partial t}$ Used to obtain w	$\frac{\partial\left(\bar{\rho}w\right)}{\partial z} = -\mathbf{\nabla}_H\cdot\left(\bar{\rho}\mathbf{v}\right)$ Used to obtain w	$\frac{\partial\left(\rho_{qs}w\right)}{\partial z} = -\mathbf{\nabla}_H\cdot\left(\rho_{qs}\mathbf{v}\right) - \frac{\partial\rho_{qs}}{\partial t}$ Used to obtain w

Equations of the Models (Cont.)

Quasi-Hydrostatic	Anelastic	Unified
N / A	$\nabla_H \cdot \left(\bar{\rho} c_p \bar{\theta} \nabla_H \pi'\right) + \frac{\partial}{\partial z}\left(\bar{\rho} c_p \bar{\theta} \frac{\partial}{\partial z} \pi'\right) = G_{AN}$ *Generally requires more iterations than the unified counterpart since π' also includes a quasi-hydrostatic component.*	$\nabla_H \cdot \left(\rho_{qs} c_p \theta \nabla_H \delta\pi\right) + \frac{\partial}{\partial z}\left(\rho_{qs} c_p \theta \frac{\partial}{\partial z} \delta\pi\right) = -\nabla_H \cdot \left(\rho_{qs} c_p \theta \nabla_H \pi_{qs}\right) + G + \frac{\partial^2 \rho_{qs}}{\partial t^2}$

Additional Models

"Anelastic" Quasi-Hydrostatic	"Anelastic" Unified
$\frac{\partial \rho_{qs}}{\partial t} = \frac{\partial^2 \rho_{qs}}{\partial t^2} = 0$	$\frac{\partial \rho_{qs}}{\partial t} = \frac{\partial^2 \rho_{qs}}{\partial t^2} = 0$

Discretization of the Equations of the Unified System

Thermodynamic equation

- Advection of potential temperature is written in a form that is consistent with the flux convergence form

Flux convergence form:

$$\frac{\partial(\rho_{qs}\theta)}{\partial t} = -\nabla_H \cdot (\theta \mathbf{v}^*) - \frac{\partial(\theta w^*)}{\partial z} + \frac{\rho_{qs} Q}{c_p \pi_{qs}} \qquad \Longrightarrow$$

Corresponding advective form:

$$\frac{\partial\theta}{\partial t} = \underbrace{\frac{1}{\rho_{qs}}\left[-\nabla_H \cdot (\theta \mathbf{v}^*) + \theta\nabla_H \cdot \mathbf{v}^*\right]}_{-\mathbf{v}\cdot\nabla_H\theta} + \underbrace{\frac{1}{\rho_{qs}}\left[-\frac{\partial(\theta w^*)}{\partial z} + \theta\frac{\partial w^*}{\partial z}\right]}_{-w\frac{\partial\theta}{\partial z}} + \frac{Q}{c_p \pi_{qs}}$$

- Discretization of horizontal mass flux $\mathbf{v}^* \equiv \rho_{qs}\mathbf{v}$ follows Takacs 3rd-order uncentered scheme
- Discretization of $\theta\mathbf{v}^*$, θw^* and w^* follows a 3rd order uncentered scheme
- Time integration scheme follows 2nd Adams-Bashforth (3rd Adams-Bashforth is an option)

Discretization of the Equations of the Unified System (Cont.)

Prediction of the quasi-hydrostatic surface exner pressure and density

- Vertical sum of the quasi-hydrostatic mass is predicted through the continuity equation.

$$\sum_{\ell=1}^{K}\left(\rho_{qs}\right)_{\ell}^{n+1}\left(\delta z\right)_{\ell}=\sum_{\ell=1}^{K}\left(\rho_{qs}\right)_{\ell}^{n}\left(\delta z\right)_{\ell}-\delta t\sum_{\ell=1}^{K}\left(\mathbf{v}^{*}\right)_{\ell}^{n}\left(\delta z\right)_{\ell}$$

- Vertical sum of the two forms of hydrostatic equations must produce the same exner pressures for the top and surface at the next time step. Then the surface exner pressure at the next time step is obtained by

$$\left(\pi_{qs}^{1/\kappa}\right)_{S}^{n+1}=\left[\left(\pi_{qs}\right)_{S}^{n+1}-\frac{g}{c_p}\sum_{\ell=1}^{K}\frac{\left(\delta z\right)_{\ell}}{\theta_{\ell}^{n+1}}\right]^{1/\kappa}+\frac{g}{p_{00}}\sum_{\ell=1}^{K}\left(\rho_{qs}\right)_{\ell}^{n+1}\left(\delta z\right)_{\ell}$$

- For internal interfaces, the exner pressures are obtained by

$$\left(\pi_{qs}\right)_{k+1/2}^{n+1}=\left(\pi_{qs}\right)_{k-1/2}^{n+1}-\frac{g}{c_p}\frac{1}{\theta_{\ell}^{n+1}}$$

- The density at the next time step

$$\left(\rho_{qs}\right)_{k}^{n+1}\equiv\frac{1}{c_p\theta_{k}^{(n+1)}}\frac{\left(p_{qs}\right)_{k-1/2}^{n+1}-\left(p_{qs}\right)_{k+1/2}^{n+1}}{\left(\pi_{qs}\right)_{k-1/2}^{n+1}-\left(\pi_{qs}\right)_{k+1/2}^{n+1}}$$

Discretization of the Equations of the Unified System (Cont.)

Computation of the nonhydrostatic exner pressure

- A simple 3D elliptic solver is used. A smoother is applied between the iteration steps to emulate the reduction process with the multigrid method.

Discretization of the first and second derivatives of density

$$\left(\frac{\partial \rho_{qs}}{\partial t}\right)^{n+1} \equiv 1.333 \times \frac{\left(\rho_{qs}\right)^{n+1} - \left(\rho_{qs}\right)^{n}}{\Delta t} - 0.333 \times \frac{\left(\rho_{qs}\right)^{n+1} - \left(\rho_{qs}\right)^{n-1}}{2\Delta t}$$

$$\left(\frac{\partial^2 \rho_{qs}}{\partial t^2}\right)^{n+1} \equiv \frac{1}{\Delta t}\left[\left(\frac{\partial \rho_{qs}}{\partial t}\right)^{n+1} - \left(\frac{\partial \rho_{qs}}{\partial t}\right)^{n}\right]$$

Discretization of the Equations of the Unified System (Cont.)

- *Horizontal and vertical grids are the C-grid and the L-grid, respectively*

Momentum equation

- Advection of momentum is written in the vector invariant form

$$\frac{D\mathbf{v}}{Dt} + f\mathbf{k} \times \mathbf{v} \quad \Longrightarrow \quad \frac{\partial \mathbf{v}}{\partial t} + q\mathbf{k} \times \mathbf{v}^* + \nabla_H K + w\frac{\partial \mathbf{v}}{\partial z}$$

- Discretization of $q\mathbf{k} \times \mathbf{v}^* + \nabla_H K$ follows Takano-Wurtale 4th order scheme
- Arakawa-Lamb and Arakawa-Hsu schemes are other options
- Arakawa-Hsu enstrophy damping procedure is included
- Discretization of $K \equiv \frac{1}{2}\mathbf{v}^2$ follows corresponding SICK-proof forms
- Discretization of horizontal mass flux $\mathbf{v}^* \equiv \rho_{qs}\mathbf{v}$ follows Takacs 3rd-order uncentered scheme
- Discretization of $w\frac{\partial \mathbf{v}}{\partial z}$ follows a 2nd order centered scheme
- Time integration scheme follows 2nd Adams-Bashforth (3rd Adams-Bashforth is an option)

Discretization of the Equations of the Unified System (Cont.)

Momentum equation

- The time integration scheme for the quasi-hydrostatic and nonhydrostatic pressure gradient force terms follows the Mesinger-Arakawa economical implicit scheme. (In the sense that the prediction of quasi-hydrostatic and nonhydrostatic exner pressure is completed before their use in the momentum equation.)

Discretization of the Equations of the Unified System (Cont.)

Computation of the vertical momentum

- The continuity equation is used to compute vertical mass flux for the next time step.

$$\left(w^*\right)_{k+1/2}^{n+1} = \left(w^*\right)_{k-1/2}^{n+1} - \left(\delta z\right)_k \left[\nabla_H \cdot \left(\mathbf{v}^*\right)^{n+1} + \left(\frac{\partial \rho_{qs}}{\partial t}\right)^{n+1}\right]$$

- At the upper and lower boundaries

$$\left(w^*\right)_S^{n+1} = \left(w^*\right)_T^{n+1} = 0$$

- Vertical velocity is

$$w_{k+1/2}^{n+1} \equiv \frac{1}{\left(\rho_{qs}\right)_{k+1/2}^{n+1}} \left(w^*\right)_{k+1/2}^{n+1}$$

Simulations of Extratropical Cyclogenesis

- Unified (UN), quasi-hydrostatic (QH) and anelastic (AN) models are used.
- Horizontal domains are midlatitude channels on β- and f-planes.
  - Domains are 5000 km long, 13000 km wide and 18 km high.
- Horizontal and vertical grid distances are 100 km and 400 m, respectively.
- Surface friction and Newtonian type cooling are included.
- Horizontal fourth-order diffusions of momentum, potential temperature are included for cosmetic reasons.

Initial Conditions for the β-Plane Simulations

Zonal Component

UNIFIED AND QUSI-HYDROSTATIC

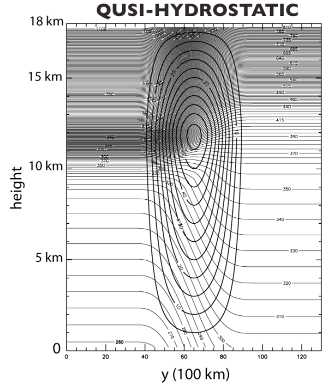

ANELASTIC

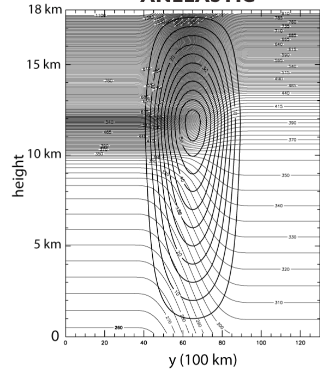

Thick lines are isotachs, thin lines are isolines of potential temperature.

- Approx. 4500 km wide single jet
- 55 m/sec maximum wind
- Nearly observed values of stability in the troposphere
- Larger than observed values of stability in the stratosphere
- Approx. 10 km high tropopause at Northern boundary
- Initial random perturbation with ±1 K magnitude is added to the potential temperature field below 10 km

Initial Conditions for the *f*-Plane Simulations

Zonal Component

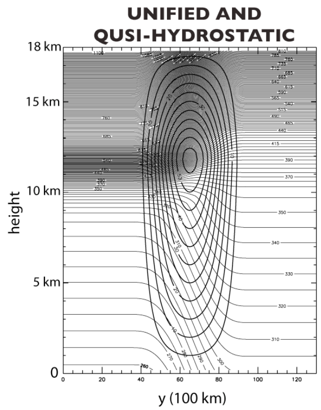

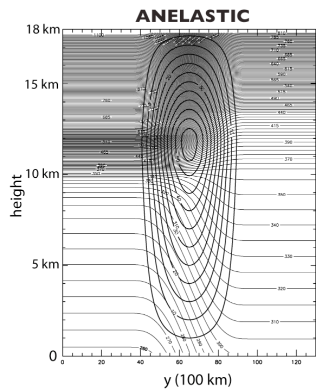

Thick lines are isotachs, thin lines are isolines of potential temperature.

Unified Model (β-Plane) Results

Surface qh-pressure (mb) and potential temperature (K) for days 9 to 19

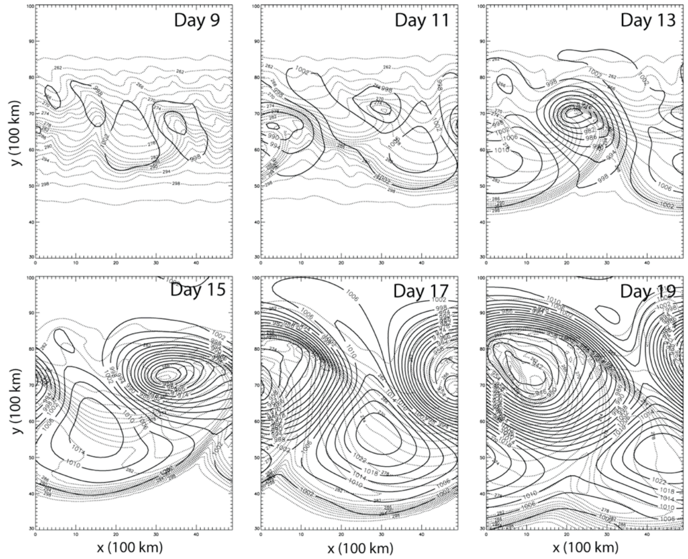

Unified Model (β-Plane) Results (Cont.)

Qh-pressure (mb) and potential temperature (K) at 5400 m for days 9 to 19

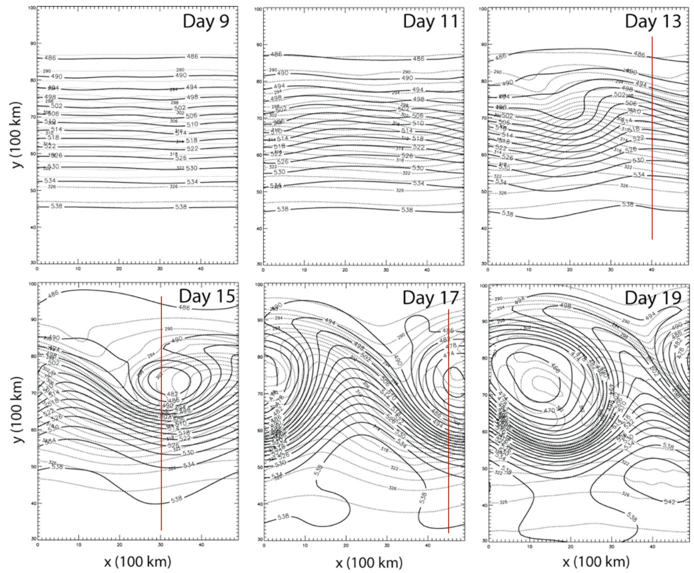

Unified Model (β-Plane) Results

- Disturbances appear to be slightly more unstable in the UN and QH simulations than that in the AN simulation

North-South Cross-Sections of Zonal Wind (m/s) and Potential Temperature (K)

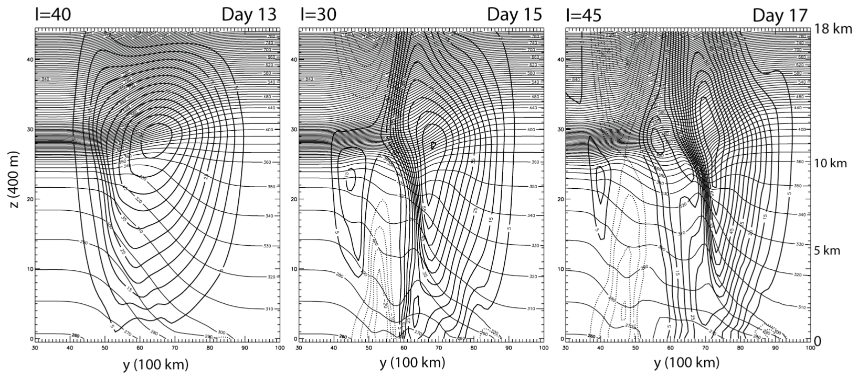

Max. wind: 56 m/s   Max. wind: 65 m/s   Max. wind: 72 m/s

Comparison of the β-Plane Results

- Nonhydrostatic effects try to compensate quasi-hydrostatic effects

Surface qh- and nh-pressure (mb) and potential temperature (K) for day 13

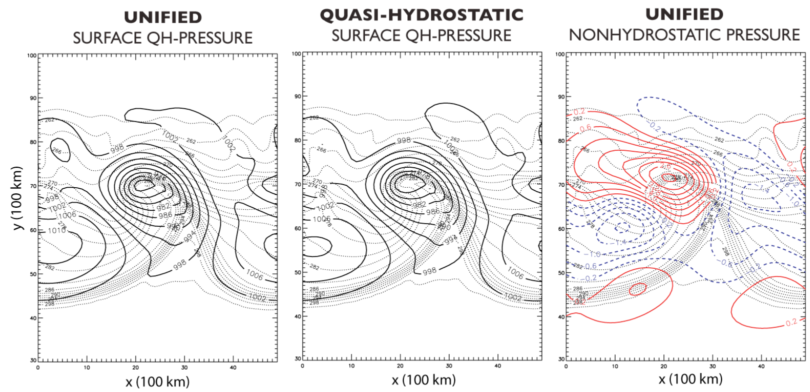

Max: 1013 mb
Min: 969 mb

Max: 1011 mb
Min: 972 mb

Max: 3.2 mb
Min: -1.9 mb

Anelastic Model (β-Plane) Results

Surface pressure (mb) and potential temperature (K) for days 9 to 19

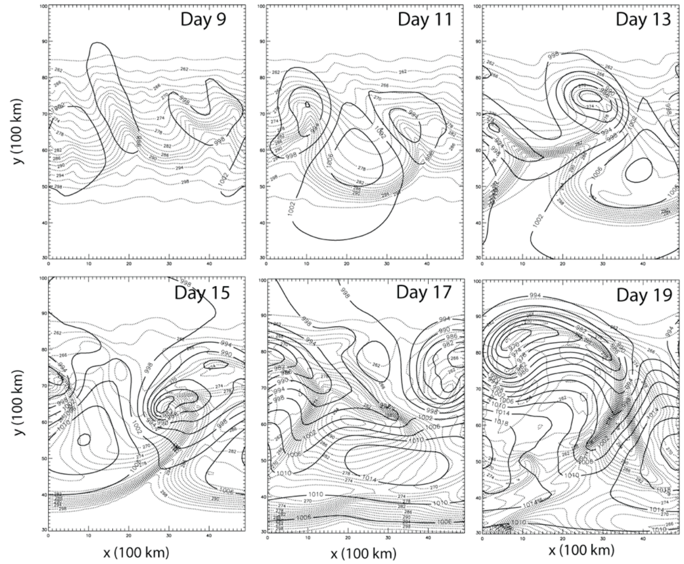

Anelastic Model (β-Plane) Results (Cont.)

Pressure (mb) and potential temperature (K) at 5400 m for days 9 to 19

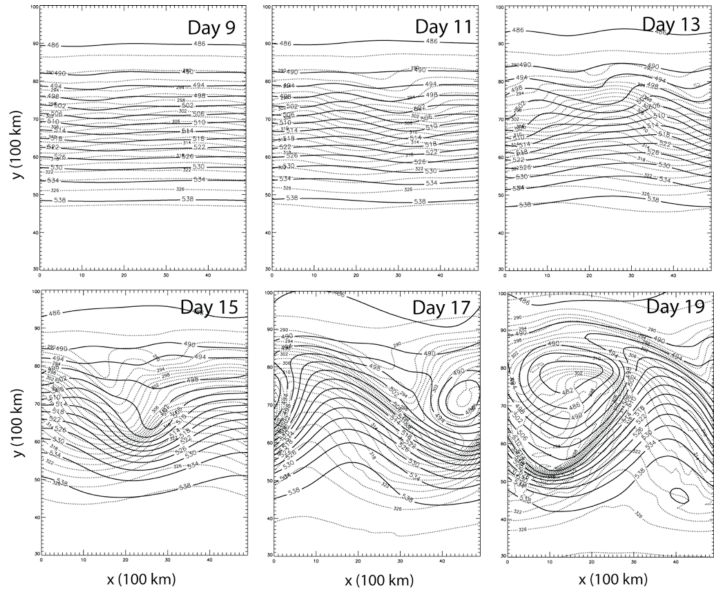

Comparison of the β-Plane Results (Cont.)

- Disturbances appear to be slightly more unstable in the UN and QH simulations than that in the AN simulation
- Yet short waves appear to be more unstable in the AN simulation than those in the UN and QH simulations

Surface qh-pressure (mb) for UN and QH (and surface pressure (mb) for AN) and potential temperature (K) for day 13

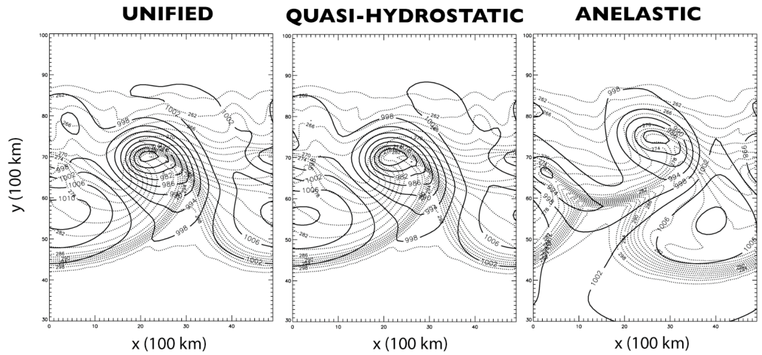

Max: 1013 mb
Min: 969 mb

Max: 1011 mb
Min: 972 mb

Max: 1011 mb
Min: 981 mb

Comparison of the β-Plane Results (Cont.)

- Yet short waves appear to be more unstable in the AN simulation than those in the UN simulation

Qh-pressure (mb) for UN and pressure (mb) for AN and potential temperature (K) at 5400 m height for day 13

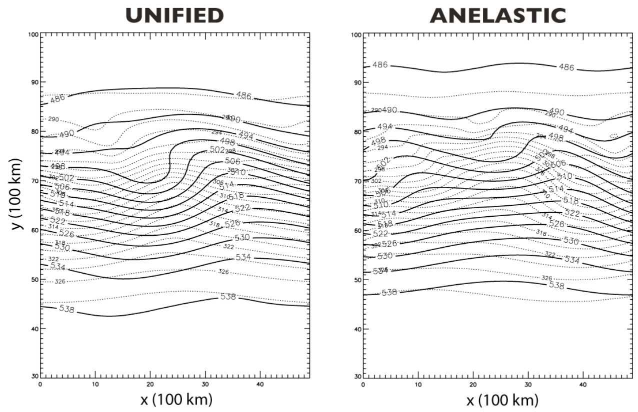

Comparison of the β-Plane Results (Cont.)

- Surface low pressure in the AN simulation does not get as deep as that in the UN and QH simulations

Surface qh-pressure (mb) for UN and QH (and surface pressure (mb) for AN) and potential temperature (K) for day 15

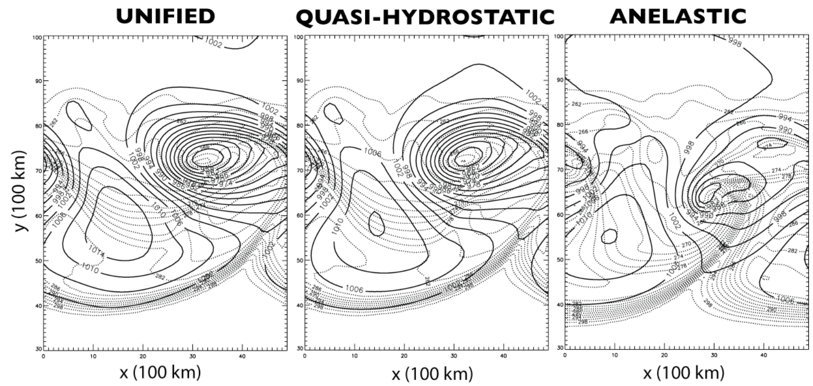

Max: 1015 mb
Min: 951 mb

Max: 1014 mb
Min: 955 mb

Max: 1014 mb
Min: 976 mb

Comparison of the *f*-Plane Results

- Disturbances appear to be more unstable in the UN simulation than that in the AN simulation

Surface qh-pressure (mb) for UN (and surface pressure (mb) for AN) and potential temperature (K) for day 13

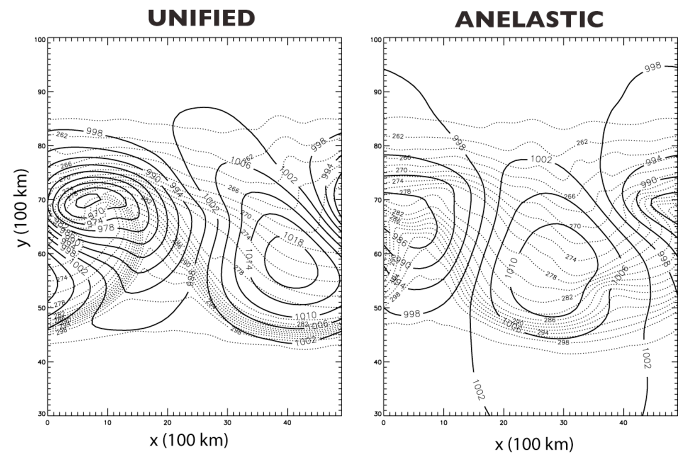

Max: 1019 mb
Min: 965 mb

Max: 1012 mb
Min: 983 mb

Comparison of the *f*-Plane Results (Cont.)

- Disturbances appear to be more unstable in the UN simulation than that in the AN simulation

Surface qh-pressure (mb) for UN (and surface pressure (mb) for AN) and potential temperature (K) for day 15

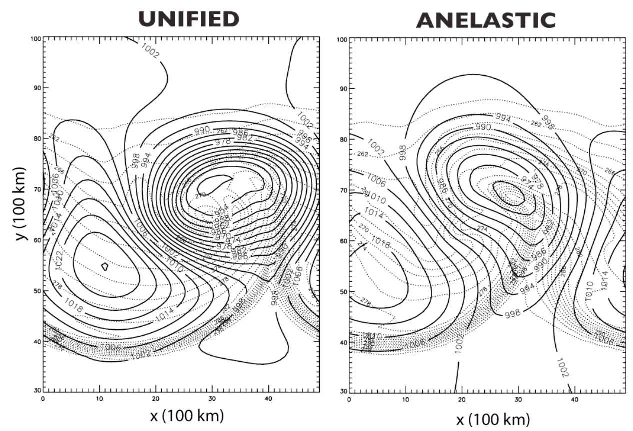

Max: 1027 mb
Min: 949 mb

Max: 1019 mb
Min: 969 mb

Conclusions

- The development of the unified dynamical core based on the height vertical coordinate and the square horizontal grid is completed.
- A comparison of the results indicates that there are differences between the UN and AN dynamical cores in simulating extratropical cyclogenesis.
- Elliptic solver needs less iterations for the UN system compared to the AN system. This is because, the elliptic solver computes only the nonhydrostatic (nh) portion of the pressure in the UN while it computes the deviation (qh + nh) from the mean for the AN system.

Continuation of Work

- The development of the unified model based on the height vertical coordinate and on the *regular hexagonal* horizontal grid